

# Preparation and Characterization of Chitosan–Zeolite Composites

W. S. Wan Ngah,<sup>1</sup> L. C. Teong,<sup>1</sup> C. S. Wong,<sup>2</sup> M. A. K. M. Hanafiah<sup>3</sup>

<sup>1</sup>*School of Chemical Sciences, Universiti Sains Malaysia, 11800 Penang, Malaysia*

<sup>2</sup>*School of Electronic Engineering, Dublin City University, Dublin 9, Ireland*

<sup>3</sup>*Department of Chemistry, Universiti Teknologi MARA Pahang, 26400 Jengka, Malaysia*

Received 15 February 2011; accepted 15 November 2011

DOI 10.1002/app.36503

Published online 22 January 2012 in Wiley Online Library (wileyonlinelibrary.com).

**ABSTRACT:** Double crosslinked chitosan–zeolite (CZ-2) and noncrosslinked chitosan–zeolite (CZ-0) composites were prepared and characterized by using Fourier transform infrared (FTIR) spectrometer, surface area analyzer, scanning electron microscope coupled with energy dispersive X-ray (SEM-EDX) spectrometer, thermogravimetric analyzer (TGA), X-ray diffraction analyzer (XRD) and carbon, hydrogen, nitrogen (CHN) analyzer. After crosslinking, CZ-2 showed a reduction in surface area and CHN content in comparison to chitosan, zeolite, and

CZ-0. Crosslinking resulted in improved stability of CZ-2 in distilled water, acetic acid and NaOH as CZ-2 recorded the lowest percentage of swelling. XRD diffractograms confirmed the formation of composites as there was a marked difference in the peak intensity at  $2\theta = 19.8^\circ$ . © 2012 Wiley Periodicals, Inc. *J Appl Polym Sci* 125: 2417–2425, 2012

**Key words:** biopolymers; characterization; chitosan; crosslinking; zeolites

## INTRODUCTION

Electroplating industry, one of the main industries, discharges a large volume of heavy metal ions into wastewater. Improper ways in removing heavy metal ions in wastewater may present a long-term risk to the ecosystem and humans. Harmful toxic heavy metal ions that are discharged by chemical industries include cadmium, mercury, lead, chromium, copper, nickel, and zinc. Pretreatment of wastewater before it is discharged into water bodies is vital to ensure the food chain is free from contaminants, thus eliminating the potential risks on humans and marine lives. Biopolymers such as chitin and chitosan have been extensively used and have become one of the emerging methods for removing heavy metal ions.<sup>1</sup> Chitosan is a type of natural polyaminosaccharide synthesized from the deacetylation of chitin, consisting predominantly of linear chains of  $\beta$ -(1 $\rightarrow$ 4)-2-acetoamido-2-deoxy-D-glucose. Chitin is the second most abundant polymer in nature after cellulose and can be extracted from

crustacean shells such as prawns, crabs, fungi, and insects.<sup>2</sup> Chitosan can be used as an adsorbent to remove heavy metals and dyes due to the presence of amino and hydroxyl groups, which can serve as the active sites.<sup>3</sup> Amino groups of chitosan can be cationized, after which they can adsorb anionic dyes strongly by electrostatic attraction in the acidic media.<sup>4</sup>

Zeolites are alumino-silicates with three-dimensional framework structure containing  $\text{AlO}_4$  and  $\text{SiO}_4$ . They are linked to each other by sharing the electrons of the oxygen, forming interconnected cages and channels.<sup>5</sup> The exchangeable cations present a counterbalance to the negative charge on the zeolite surface which is generated from the isomorphous substitution.<sup>6</sup> Recently, the use of natural zeolite has gained much interest in adsorption studies due to its good sorption properties and easy modification capability.<sup>7</sup> From the literatures, chitosan was able to form composites with perlite,<sup>8,9</sup> sand,<sup>8,10</sup> and bentonite.<sup>8,11,12</sup> Natural zeolite,<sup>13</sup> zeolite NaX,<sup>14</sup> and Y zeolite<sup>15</sup> have been used to adsorb heavy metals. Therefore, chitosan and zeolite are the promising materials to be used as adsorbents. Despite the great interest in using zeolite or chitosan as adsorbent, to our knowledge the development of composites using both chitosan and zeolite is scarce. Limited data regarding this field has restricted the development of this composite. Hence, developing a composite by using zeolite and chitosan will allow further exploration into the possibility of using the composite as an

Correspondence to: W. S. Wan Ngah (wsaime@usm.my).

Contract grant sponsor: Universiti Sains Malaysia; contract grant numbers: 1001/PKIMIA/822115, 1001/PKIMIA/843051.

Contract grant sponsor: Universiti Sains Malaysia Fellowship.

absorbent. The objective of this study was to prepare and to synthesize the composite beads from chitosan and zeolite by crosslinking them with epichlorohydrin and sodium tripolyphosphate.

## EXPERIMENTAL

### Materials

Medium molecular weight chitosan with the degree of deacetylation of 75–85% and zeolite with particle size  $< 45 \mu\text{m}$  was supplied by Sigma-Aldrich. All the reagents used were of analytical-reagent grade, and distilled water was used throughout this study.

### Preparation of the composites

#### Chitosan beads

Chitosan beads were prepared based on the method proposed by Wan Ngah and Fatinathan.<sup>16,17</sup> First, chitosan solution was prepared by dissolving 2.0 g chitosan in 60 mL (5%, v/v) acetic acid solution. After that, the viscous solution was left overnight to ensure complete dissolution of chitosan flakes. The chitosan gel solution was then added dropwise into a precipitation bath containing 500 mL (0.50M) NaOH and stirred at 200 rpm. The beads were filtered, rinsed with distilled water to remove excess NaOH and air-dried. Finally, the chitosan beads were ground using mortar and sieved to obtain the desired size ( $< 200 \mu\text{m}$ ). Hereafter, the beads were called chitosan beads (CB).

#### Non-crosslinked chitosan–zeolite composite

The noncrosslinked chitosan–zeolite composite was prepared by mixing chitosan and zeolite under room temperature (25°C) as follows: 4 g chitosan and 4 g zeolite were mixed in 160 mL (5%, v/v) acetic acid. The suspension was stirred vigorously for 2 h. A 100 mL of 5% acetic acid was added into the suspension and stirred vigorously for 1 h. The suspension was added dropwise into the precipitation bath containing 500 mL (0.50M) NaOH. The mixture was stirred at 100 rpm for 3 h. The beads formed were filtered and washed with distilled water to remove excess NaOH. Finally, the beads were air dried before grinding to obtain the desired size ( $< 200 \mu\text{m}$ ). The newly prepared noncrosslinked chitosan–zeolite composite is hereafter called CZ-0.

#### Double crosslinked chitosan–zeolite composite

Double crosslinked chitosan–zeolite composite beads were prepared by mixing chitosan and zeolite under room temperature (25°C) as follows: 4 g chitosan and 4 g of zeolite were mixed in 160 mL (5% v/v)

acetic acid. The suspension was stirred vigorously for 2 h. A 160 mL (0.01M) epichlorohydrin (ECH) with pH 10.0 was then added into the suspension and stirred vigorously for another 1 h. The suspension was added dropwise into the precipitation bath containing 500 mL (0.05M) sodium tripolyphosphate (NaTPP). The mixture was stirred at 100 rpm for 3 h. Beads formed in the solution bath were filtered, and washed with distilled water to remove excess NaTPP. Finally, the beads were air-dried before grinding using mortar to the desired size ( $< 200 \mu\text{m}$ ). The newly prepared crosslinking chitosan–zeolite composite is hereafter called CZ-2.

#### Characterization of CZ-0 and CZ-2

To determine the physical and chemical changes that took place on CZ-0 and CZ-2, the composites were characterized by spectroscopic and quantitative analyses. The results were also compared with chitosan and zeolite.

#### Functional groups identification

The functional groups present in chitosan, zeolite, and chitosan–zeolite composites were recorded by using Fourier transform infrared (FTIR) spectrometer (PerkinElmer, System 2000 Model). The spectra were recorded in the wavenumber range from 4000 to 400  $\text{cm}^{-1}$  by KBr pellet technique.

#### Surface area and average pore diameter analysis

The BET and Langmuir surface areas (based on BET and Langmuir isotherm plots), and average pore diameter were determined by using a Micromeritics ASAP 2010 gas adsorption surface analyzer. The Micromeritics ASAP 2010 instrument operating using nitrogen intrusion technique.

#### Carbon, hydrogen, and nitrogen analysis

Elemental analysis on chitosan and chitosan–zeolite composite was carried out by using CHN/O analyzer (PerkinElmer, Series II CHNS/O Analyzer 2400). The analysis was carried out at the combustion temperature of 925°C and reduction temperature of 640°C.

#### Thermogravimetric analysis

The mass loss of chitosan, zeolite, and chitosan–zeolite composites as a function of temperature was determined by a thermogravimetric analyzer or TGA (PerkinElmer TGA 7). A weight of about 10.0 mg of each sample was combusted in oxygen at a rate of 20°C  $\text{min}^{-1}$  until a final temperature of 900°C was

reached. The results were plotted as a function of percentage weight loss and derivative weight loss versus temperature.

### Surface morphology analysis

The surface morphology of chitosan-zeolite composites was observed by using a scanning electron microscope (SEM, Leo Supra 50VP, Carl Zeiss SMT) coupled with energy dispersive X-ray (EDX) spectrometer. The samples were coated with gold by a Polaron SC 515 sputter coater prior to analysis in order to increase the conductivity of the samples.

### X-ray diffraction

X-ray diffractograms of chitosan, zeolite and chitosan-zeolite composites were obtained by using an X-ray diffractometer. A Rigaku RINT-2100 rotating anode XRD system generating monochromated CuK $\alpha$  radiation with a continuous scanning mode at a rate of 0.05 min<sup>-1</sup> and operating conditions of 40 kV and 30 mA was used to obtain XRD pattern. Samples were scanned in the range 5° < 2 $\theta$  < 60°.

### Solubility and swelling tests

The solubility of chitosan, zeolite, and chitosan-zeolite composites was tested in 5% (v/v) acetic acid, 0.10M NaOH and distilled water. Approximately 0.05 g of the samples was added into 50 mL of each solution and was left stirring for 24 h. The solubility of the beads in these solutions was observed and recorded after 24 h. The swelling of chitosan, zeolite,

and chitosan-zeolite composites was also tested in these three solutions. About 0.05 g of the beads was transferred into a glass tube with a diameter of 5 mm and a height of 100 mm. The levels of the beads were marked before filling the glass tube with 1 mL (5% v/v) acetic acid, 0.10M NaOH, or distilled water and were left for 24 h. The height of the beads in all three solutions was obtained. The percentage of swelling was calculated using the following equation<sup>18,19</sup>:

$$S = \left( \frac{h_t - h_o}{h_o} \right) \times 100 \quad (1)$$

where  $S$  is the percentage of swelling (%),  $h_t$  is the height of swollen beads (cm) at the time  $t$  and  $h_o$  is the initial height of the beads (cm).

## RESULTS AND DISCUSSION

### Functional groups identification

From the FTIR spectrum of zeolite (Fig. 1), the broad peak at 3413 cm<sup>-1</sup> indicates the stretching vibration of hydroxyl in zeolite. The peak at wavenumber 1661 cm<sup>-1</sup> represents H-O-H bending vibration, 1005 cm<sup>-1</sup> for Si-O stretching vibration, 556 cm<sup>-1</sup> and 463 cm<sup>-1</sup> correspond to Al-O-Si and Si-O-Si bending vibrations, respectively. FTIR spectrum of chitosan shows a much broader peak at 3429 cm<sup>-1</sup>, corresponding to greater number of stretching vibration of the hydroxyl group. The vibration band at 2882 cm<sup>-1</sup> is due to the C-H stretching vibration of O-CH-O. The peak at wavenumber 1648 cm<sup>-1</sup>

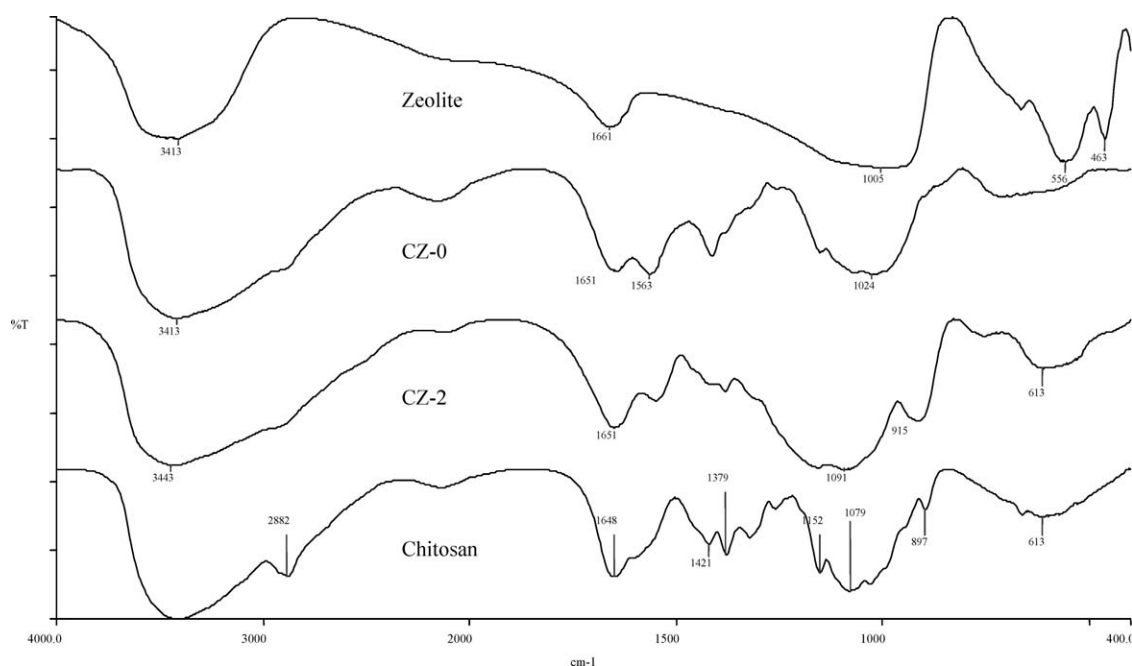


**Figure 1** FTIR spectra of zeolite, CZ-0, CZ-2 and chitosan.

**TABLE I**  
BET and Langmuir Surface Areas and Average Pore Diameters of Chitosan, Zeolite, CZ-0, and CZ-2

Adsorbent	BET surface area (m <sup>2</sup> /g)	Langmuir surface area (m <sup>2</sup> /g)	Average pore diameter (nm)
Chitosan	0.98	1.76	63.01
Zeolite	0.75	1.17	110.56
CZ-0	1.72	1.09	94.25
CZ-2	0.77	1.26	99.94

indicates the deformation vibration of NH<sub>2</sub>, 1421 cm<sup>-1</sup> and 1379 cm<sup>-1</sup> for C—H bending vibrations, 1152 cm<sup>-1</sup> for asymmetry C—O—C stretching vibrations of CH—O—CH and 1079 cm<sup>-1</sup> for C—O stretching vibration of CH—OH.

CZ-0 and CZ-2 showed a small shift in wavenumber of NH<sub>2</sub> deformation vibration peak compared to the FTIR spectrum of chitosan. For CZ-0, the peak indicating the presence of NH<sub>2</sub> group (1651 cm<sup>-1</sup>) is smaller in percentage of transmittance compare to the NH<sub>3</sub><sup>+</sup> deformation vibration peak (1563 cm<sup>-1</sup>).

**TABLE II**  
Percentage of Carbon, Hydrogen, and Nitrogen and the C/N Ratio for Chitosan, CZ-0, and CZ-2

Adsorbent	C (%)	H (%)	N (%)	C/N
Chitosan	37.51	6.12	6.53	5.74
CZ-0	19.15	4.43	2.87	6.67
CZ-2	15.88	4.10	2.71	5.86

Chitosan–zeolite composites exhibited the characteristics of both chitosan and zeolite. The peaks at 1024 cm<sup>-1</sup> (CZ-0) and 1091 cm<sup>-1</sup> (CZ-2) represent the stretching vibrations of Si—O group. The peak at 712 cm<sup>-1</sup> in CZ-0 represents the stretching vibration of Si—C while the peak at 613 cm<sup>-1</sup> in CZ-2 represents Si—O—Si stretching vibration. The presence of Si—C peaks indicated the presence of bonding between chitosan and zeolite. CZ-2 has an extra peak at 915 cm<sup>-1</sup>, indicating the stretching vibration of P—O—P. This was due to the addition of the second crosslinking agent (TPP) into the composite. From the FTIR spectra, the addition of crosslinking agent has reduced the number of C—H sites as the peak that

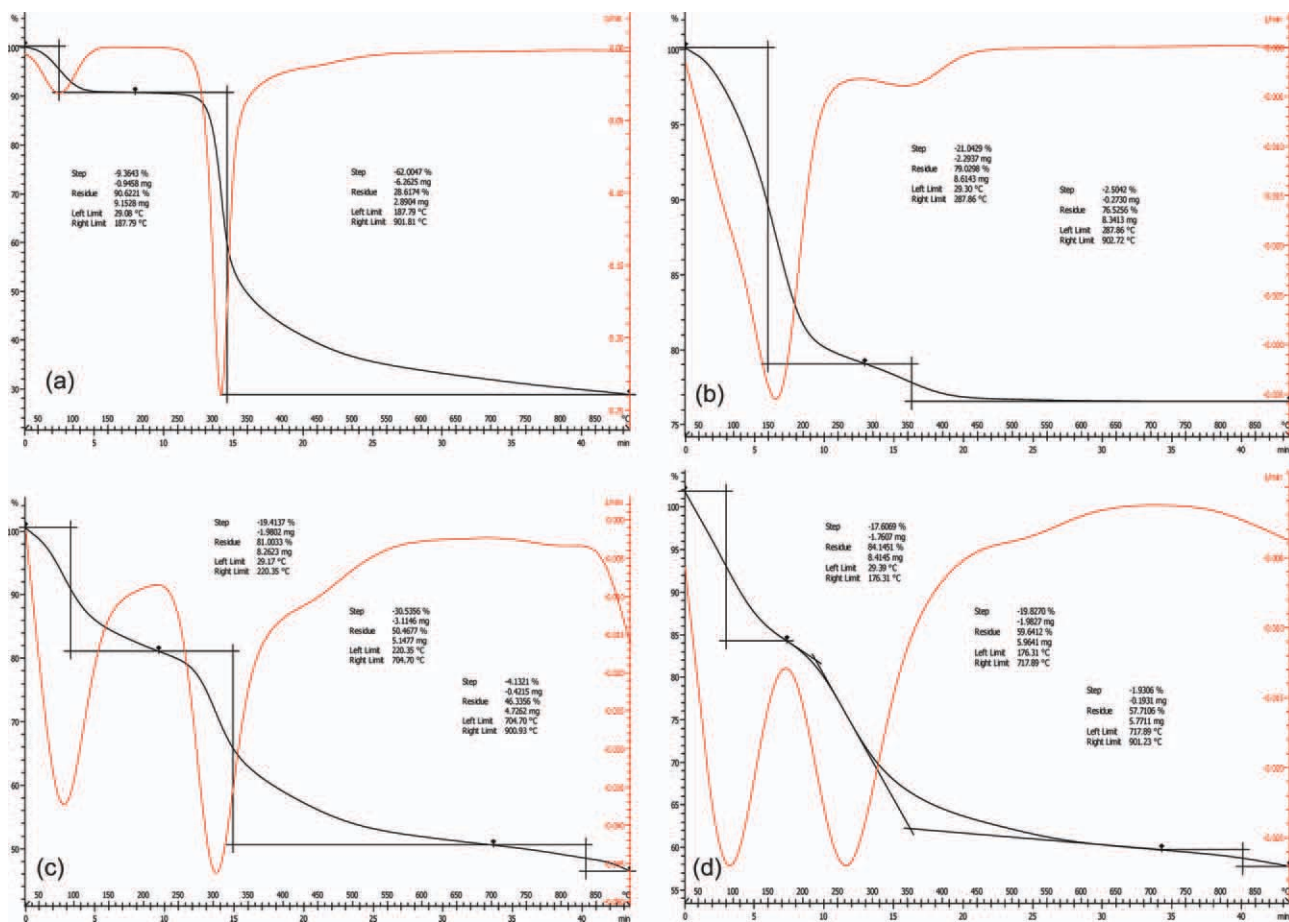


**Figure 2** (a) Thermogravimetric curve of chitosan. (b) Thermogravimetric curve of zeolite. (c) Thermogravimetric curve of CZ-0. (d) Thermogravimetric curve of CZ-2. [Color figure can be viewed in the online issue, which is available at [wileyonlinelibrary.com](http://wileyonlinelibrary.com).]

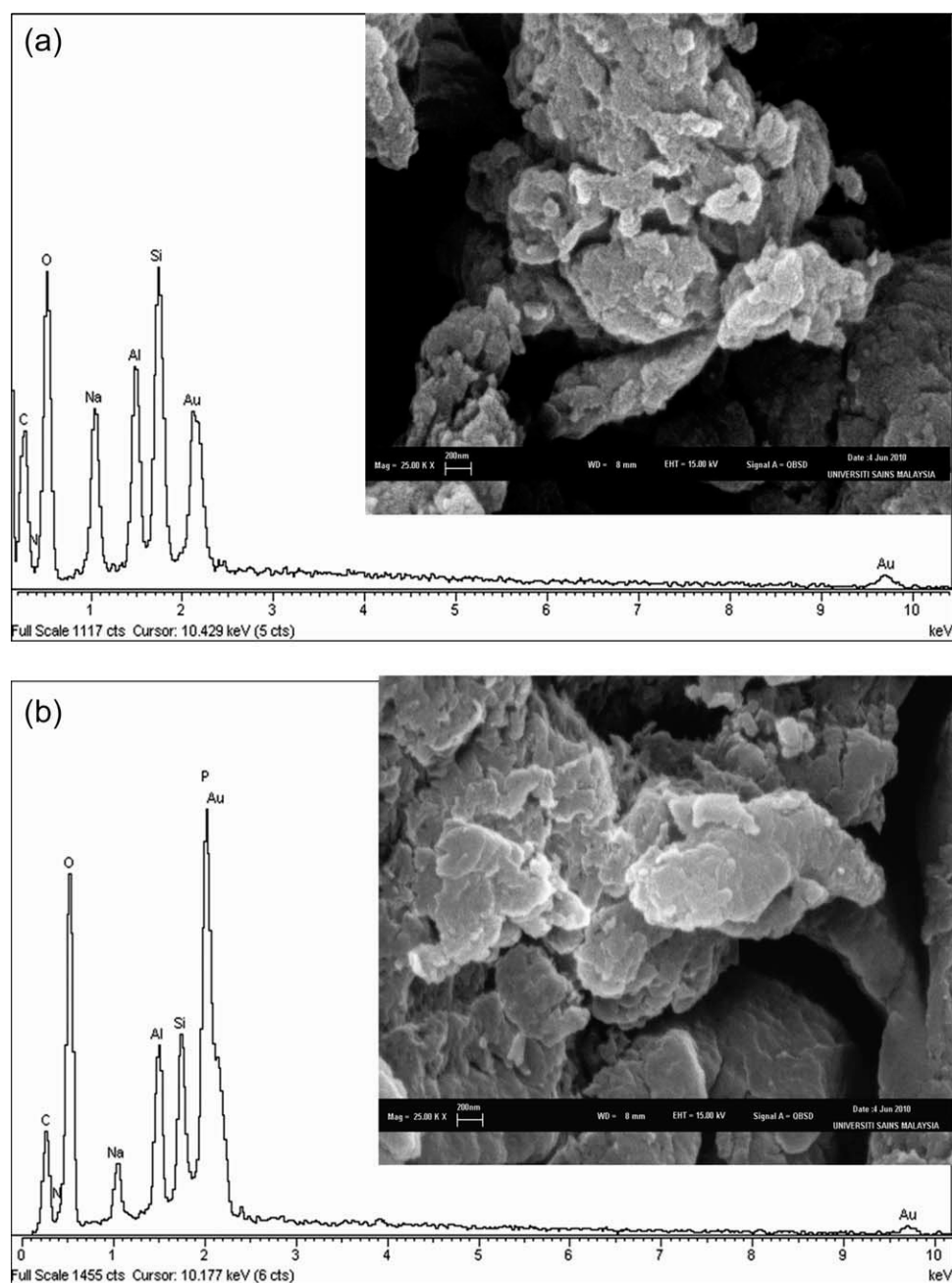


**Figure 3** (a) SEM images and EDX spectra of CZ-0 at 25,000 $\times$  magnification. (b) SEM images and EDX spectra of CZ-2 at 25,000 $\times$  magnification.

represents the C–H bending vibrations ( $1421\text{ cm}^{-1}$ ) is getting weaker as more crosslinking agent is added into the composites.

#### Surface area and average pore diameter analysis

Table I shows the values of BET and Langmuir surface areas and average pore diameters for chitosan, zeolite, CZ-0, and CZ-2. According to the International Union of Pure and Applied Chemistry (IUPAC) recommendations, the micropores are defined as pores with diameter not exceeding 2 nm,

mesopores are pores with diameter between 2 and 50 nm, and macropores represent pores with diameter greater than 50 nm.<sup>20</sup> On the basis of Table I, all the four materials have an average pore diameter greater than 50 nm, indicating the presence of macropores. This indicates that the pores are so wide, that it is virtually impossible to map out the isotherm in detail because the relative pressures are so close to unity.<sup>20</sup> The average pore diameter of CZ-0 and CZ-2 is in between chitosan and zeolite. The results showed that crosslinking process has increase the average pore size of CZ-2. After crosslinking,

chitosan molecules were packed in the interlayer of zeolite, which resulted in pore blockage that inhibited the adsorption of nitrogen molecules. Entrapment of chitosan with zeolite was caused by the bridging mechanisms and interactions of the hydroxyl group at the surface of zeolite with each other.<sup>11</sup> The both composites (CZ-0 and CZ-2) are having the BET surface area approximately same as zeolite, indicating that the chitosan is entrapped in the zeolite and not the other way round.

### Carbon, hydrogen, and nitrogen analysis

Carbon, hydrogen, and nitrogen (CHN) elemental analysis results for chitosan, CZ-0 and CZ-2 are summarized in Table II. CZ-0 and CZ-2 showed an increase in the C/N ratio compared to chitosan. However, crosslinking had a small effect on the C/N ratio as in the case of CZ-2. An increase in the number of crosslinking agents (ECH and TPP) resulted in a further reduction in the percentages of CHN. The crosslinking (ECH and TPP) had resulted in a further reduction in the percentages of CHN. The nitrogen of the amine groups in chitosan were involved in the crosslinking reaction between chitosan and TPP and also chitosan with negative surface of zeolite. Hence the decrease in the nitrogen percentage is due to the unavailability of free pendant amine groups of chitosan polymer. The decrease in the percentage of nitrogen in the chitosan zeolite composite indicated successful crosslinking and entrapment process.<sup>21</sup>

### Thermogravimetric analysis

Thermogravimetric curves of CZ-0, CZ-2, chitosan, and zeolite are illustrated in Figure 2. For chitosan [Fig. 2(a)], two decomposition temperatures can be noticed. The initial weight loss of 9.37% from room temperature (30°C) to 188°C corresponds to the release of adsorbed water. The second decomposition region (250–900°C) recorded the maximum weight loss of chitosan where chitosan would be dissociated and totally burned out<sup>11,12,22,23</sup> leaving 28.61% residue. As for zeolite [Fig. 2(b)], the first decomposition (30–300°C) exhibited the major weight loss of 20.97% which is due to the release of adsorbed water. The second weight loss (300–900°C) involved a small loss of the hydroxyl structure in zeolite, with 76.52% residue remained as metal oxides. For CZ-0 [Fig. 2(c)], 19% of water loss was recorded from 30 to 180°C. This was followed by the decomposition of chitosan at 250 to 450°C. For CZ-2 [Fig. 2(d)], the first weight loss (30–180°C) also represents the loss of adsorbed water, followed by the decomposition of chitosan at higher temperatures (200–450°C). The percentage of residue left in CZ-2 is

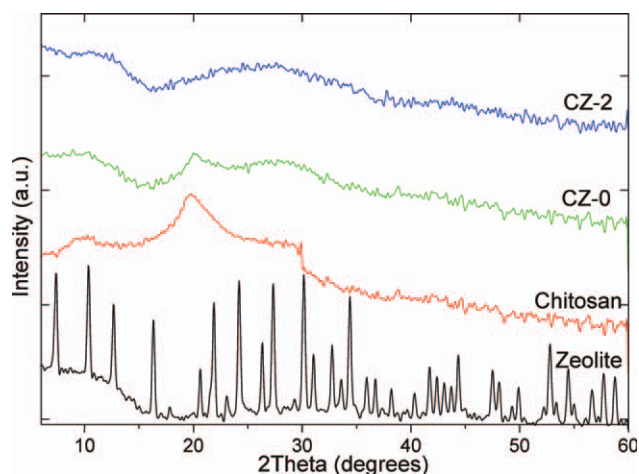


**Figure 4** XRD diffractograms of chitosan, CZ-0, CZ-2, and zeolite. [Color figure can be viewed in the online issue, which is available at [wileyonlinelibrary.com](http://wileyonlinelibrary.com).]

much higher than in CZ-0. This shows that CZ-2 contains more minerals compared with CZ-0 as the crosslink agent (NaTPP) was involved in binding zeolite during the formation of the composite.

### Surface morphology

The SEM images showed that the chitosan–zeolite composites (Fig. 3) have a rough and irregular surface. On the basis of the EDX spectra, sodium is detected, which might have originated from sodium hydroxide and zeolite where the sodium ions counterbalanced the negative charge of zeolite.<sup>6</sup> The presence of carbon, nitrogen, oxygen, aluminum, and silicon in CZ-0 and CZ-2 was also detected. As for CZ-2, there is an additional peak (P) which is not observed in CZ-0. The presence of phosphorus was due to the addition of NaTPP as the second crosslink agent. The presence of silicon and aluminum in CZ-0 and CZ-2 confirms the formation of chitosan–zeolite composites. The presence of gold peaks (Au) in all spectra is due to the gold purposely settled to enhance electric conduction in order to improve the quality of the images.

### X-ray diffraction

X-ray diffraction (XRD) diffractograms of chitosan, zeolite, and chitosan–zeolite composites are shown in Figure 4. The characteristic peaks of chitosan are displayed by the peaks  $2\theta = 9.8$  and  $19.8$ .<sup>22,23</sup> Such pattern characterized a chitosan polymorph, which is referred to in literature as the “tendon” hydrated polymorph.<sup>24</sup> From Figure 4, the main difference observed between the diffractograms obtained for chitosan and CZ-0 and CZ-2 is the inversion of the relative diffracted intensity of the peaks at  $2\theta = 19.8^\circ$ . Chitosan has a much higher intensity

**TABLE III**  
**Dissolution and Swelling Percentage of Chitosan, Zeolite, CZ-0, and CZ-2 in 5% (v/v) Acetic Acid, Distilled Water, and 0.10M NaOH**

Adsorbent	5% (v/v) Acetic acid		Distilled water		0.10M NaOH	
	Solubility	Swelling (%)	Solubility	Swelling (%)	Solubility	Swelling (%)
Chitosan	Soluble	-	Insoluble	113.1 ± 0.5	Insoluble	74.1 ± 1.6
Zeolite	Soluble	-	Insoluble	0	Insoluble	0
CZ-0	Insoluble	100.0 ± 0.0	Insoluble	0	Insoluble	20.0 ± 0.0
CZ-2	Insoluble	20.0 ± 0.0	Insoluble	0	Insoluble	0

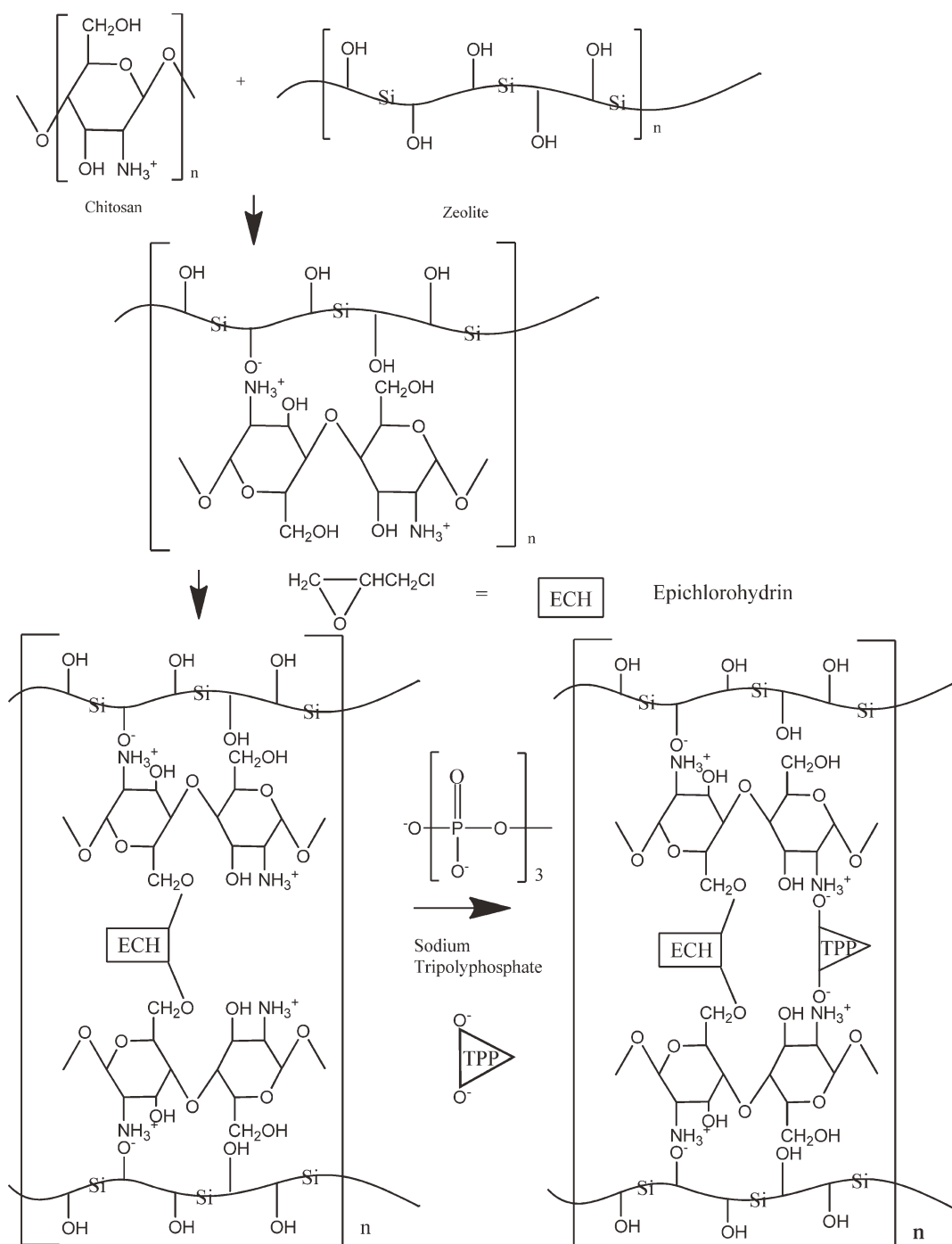


**Figure 5** Proposed structure of chitosan-zeolite composites.

compared to CZ-0 while in CZ-2 this peak has disappeared, indicating structural changes in chitosan during the formation of composites. This is due to the highly disorder intercalation between chitosan and zeolite.<sup>25,26</sup> The peak position is slightly shifted to higher diffraction angles, hence decreases the basal spacing, which indicates the formation of composites between chitosan and zeolite.<sup>27</sup> This phenomenon has been described in literature suggesting the possibility of the destruction of the hydrogen bonding between the amino and the hydroxyl group in chitosan after crosslinking had occurred.<sup>28</sup>

### Solubility and swelling test of chitosan and chitosan-zeolite composite

The solubility of chitosan, CZ-0, CZ-2, and zeolite in 5% (v/v) acetic acid, 0.10M NaOH and distilled water is shown in Table III. Chitosan was found to be insoluble in distilled water and in NaOH solution; however, chitosan dissolved in acetic acid solution and produced a viscous solution. This was due to the protonation of the amine groups (forming  $-\text{NH}_3^+$ ) in chitosan at low pH. Protonation of the amine groups would result in the destruction of the polymer chain followed by dissolution of the polymer. Chitosan did not dissolve in distilled water and NaOH solution because the amount of proton ( $\text{H}^+$ ) present causes protonation of the amine groups of chitosan to be much lower.

Crosslinking in CZ-2 has successfully overcome the instability of chitosan and CZ-0 that tend to dissolve in acetic acid and change the crystalline nature of the composite (Table III). CZ-2 composite did not dissolve in all three solutions; however, it exhibits 20% of swelling in 5% acetic acid. The percentage of swelling of CZ-2 composite is much lower than CZ-0. The swelling ability of chitosan-zeolite composites is dependent on the degree of crosslinking. This agrees with the literature that at higher crosslinking density, the percentage of swelling will be much lower.<sup>29</sup> However, in this study, swelling could still be observed in the composites, indicating that the degree of crosslinking is not enough to prevent the dissolution of the composite. Results showed that crosslinking had improved the chemical stability of the composites as the beads were not completely dissolved.

### Proposed structure

Zeolite has a negative surface, which is counterbalanced by sodium or potassium cations. The negative surface of the zeolite tends to bind to the protonated amine site of chitosan. When the first crosslink agent (ECH) was introduced, the ring structure of the ECH was broken and formed a bridge that linked two chitosan molecules together. This was proven

by the presence of the peak at  $1152\text{ cm}^{-1}$ , indicating the C—O—C stretching vibration. After the second crosslink agent (TPP) was introduced, the TPP, which contained  $\text{O}^-$  negative site, was attracted to the protonated amino group in chitosan. TPP also formed bridges that linked two chitosan molecules together. From the FTIR spectra (Fig. 1), the peak that indicated  $\text{NH}_3^+$  group in CZ-0 and CZ-2 was clearly seen at  $1563\text{ cm}^{-1}$ . The FTIR spectra obtained in this work were also similar to the FTIR patterns reported in the literature.<sup>30,31</sup> The equations for the formation of chitosan-zeolite composites are given in Figure 5.

### CONCLUSION

The characteristics of chitosan-zeolite composites were revealed through various analyses that include FTIR, BET, TGA, SEM-EDX, XRD, and CHN. BET studies showed that the composites consist of macropores since the average pore diameter is greater than 50 nm. TGA analysis revealed different decomposition profiles for chitosan, zeolite, CZ-0, and CZ-2, an indication that different components were present in each of the compounds. CZ-2 recorded higher percentage of residue compared with CZ-0 because CZ-2 contains more metal oxides at high temperature. On the basis of the XRD patterns, the basal spacing decreased as the peak shifted to higher angles, suggesting the changes in the active site of the composites. CHN analysis shows that CZ-0 records a higher C/N ratio compared with CZ-2, an indication that CZ-0 contains more  $\text{NH}_3^+$  active site than CZ-2.

### References

1. Crini, G. *Bioresour Technol* 2006, 97, 1061.
2. Wan Ngah, W. S.; Isa, I. M. *J Appl Polym Sci* 1998, 67, 1067.
3. Wu, F.-C.; Tseng, R.-L.; Juang, R.-S. *J Hazard Mater* 2001, 81, 167.
4. Ravi Kumar, M. N. V. *React Funct Polym* 2000, 46, 1.
5. Englert, A. H.; Rubio, J. *Int J Miner Process* 2005, 75, 21.
6. Motsi, T.; Rowson, N. A.; Simmons, M. J. H. *Int J Miner Process* 2009, 92, 42.
7. Cincotti, A.; Mameli, A.; Locci, A. M.; Orrù, R.; Cao, G. *Ind Eng Chem Res* 2005, 45, 1074.
8. Wan Ngah, W. S.; Teong, L. C.; Hanafiah, M. A. K. M. *Carbohydr Polym* 2011, 83, 1446.
9. Hasan, S.; Ghosh, T. K.; Viswanath, D. S.; Boddu, V. M. *J Hazard Mater* 2008, 152, 826.
10. Wan, M.-W.; Kan, C.-C.; Rogel, B. D.; Dalida, M. L. P. *Carbohydr Polym* 2010, 80, 891.
11. Futralan, C. M.; Kan, C. C.; Dalida, M. L.; Hsien, K. J.; Pascua, C.; Wan, M. W. *Carbohydr Polym* 2011, 83, 528.
12. Futralan, C. M.; Kan, C. C.; Dalida, M. L.; Pascua, C.; Wan, M. W. *Carbohydr Polym* 2011, 83, 697.
13. Peric, J.; Trgo, M.; Vukojevic Medvidovic, N. *Water Res* 2004, 38, 1893.
14. Svilovic, S.; Rusic, D.; Stipisic, R. *J Hazard Mater* 2009, 170, 941.



15. Keane, M. A. *Colloid Surf A-Physicochem Eng Asp* 1998, 138, 11.
16. Wan Ngah, W. S.; Fatinathan, S. *Colloid Surf A-Physicochem Eng Asp* 2006, 277, 214.
17. Wan Ngah, W. S.; Fatinathan, S. *J Environ Manage* 2010, 91, 958.
18. Ostrowska-Czubenko, J.; Gierszewska-Druzynska, M. *Carbohydr Polym* 2009, 77, 590.
19. Rivero, S.; García, M. A.; Pinotti, A. *Carbohydr Polym* 2010, 82, 270.
20. Gregg, S. J.; Sing, K. S. W. *Adsorption, Surface Area and Porosity*; Academic Press: New York, 1982.
21. Monteiro, O. A. C. Jr; Airoidi, C. *Int J Biol Macromol* 1999, 26, 119.
22. Jaworska, M.; Sakurai, K.; Gaudon, P.; Guibal, E. *Polym Int* 2003, 52, 198.
23. Yang, X.; Tu, Y.; Shang, S.; Tao, X. *App Mater Interfaces* 2010, 6, 1707.
24. Belamie, E.; Domard, A.; Giraud-Guille, M. M. *J Polym Sci Part A: Polym Chem* 1997, 35, 3181.
25. Kittinaovarat, S.; Kansomwan, P.; Jiratumnukul, N. *Appl Clay Sci* 2010, 48, 87.
26. Wang, L.; Wang, A. *J Hazard Mater* 2007, 147, 979.
27. Monvisade, P.; Siriphannon, P. *Appl Clay Sci* 2009, 42, 427.
28. Wan Ngah, W. S.; Ariff, N. F. M.; Hashim, A.; Hanafiah, M. A. K. M., *Clean-Soil Air Water* 2010, 38, 394.
29. Lee, S.-T.; Mi, F.-L.; Shen, Y.-J.; Shyu, S.-S. *Polymer* 2001, 42, 1879.
30. Dogan, H.; Durmaz Hilmioglu, N. *Desalination* 2010, 258, 120.
31. Kittur, A. A.; Kulkarni, S. S.; Aralaguppi, M. I.; Kariduraganavar, M. Y., *J Membr Sci* 2005, 247, 75.